PROCEEDINGS OF SCIENCE

Electron bremsstrahlung recovery in ATLAS tracking using Dynamic Noise Adjustment

Evelina Bouhova-Thacker, Vakhtang Kartvelishvili*
Lancaster University, UK (on behalf of ATLAS collaboration)
E-mail: vakhtang.kartvelishvili@cern.ch

A number of approaches are being used in ATLAS reconstruction software, aiming to improve electron momentum measurement by taking into account the effects due to bremsstrahlung at various stages. One of them, designed and implemented in ATLAS, is covered in this talk. The method applies Dynamic Noise Adjustment (DNA) during the track fitting process based on the Kalman filter, and is both fast and efficient.

XI International Workshop on Advanced Computing and Analysis Techniques in Physics Research
April 23-27 2007
Amsterdam, the Netherlands

*Speaker.

PoS(ACAT)046

1. Introduction

Various physics channels to be used for physics studies by the ATLAS collaboration at the LHC — Higgs and supersymmetry searches, B-hadron and quarkonium physics and many others — require effi cient detection and precise measurement of electrons and positrons produced in proton-proton collisions. High precision silicon detectors, transition radiation detectors and electromagnetic calorimeters are used for this purpose in the ATLAS detector (see fi g. 1 and ref. [1] for details).

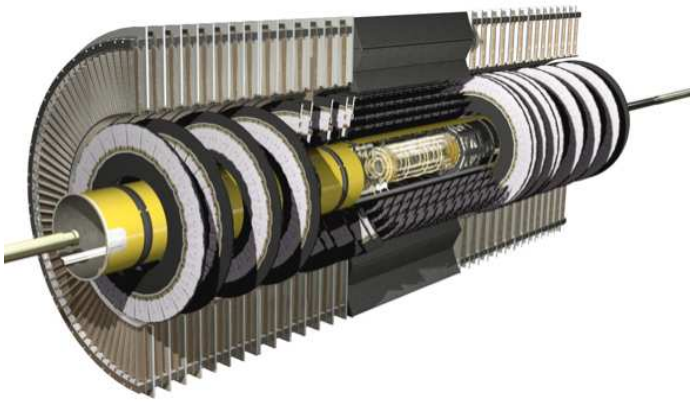

Figure 1: *Schematic view of the ATLAS Inner Detector.*

However, the amount of material being traversed by the electrons propagating through the ATLAS inner detector (ID), shown in fi g. 2, is not negligible. In particular, particles emerging

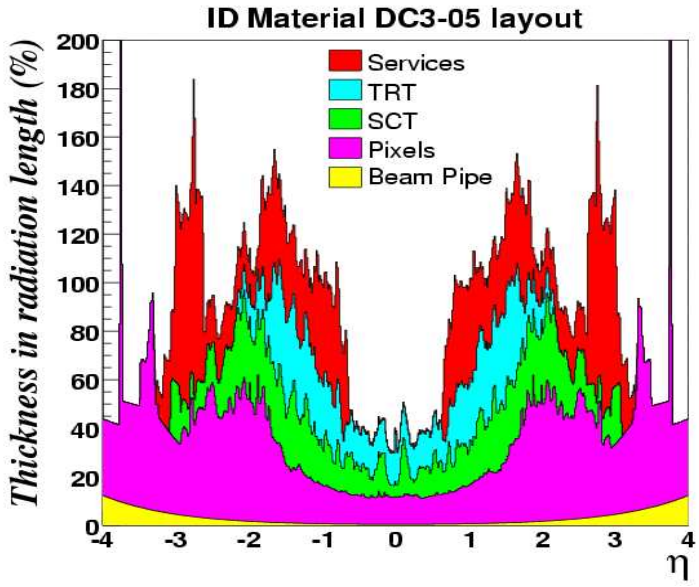

Figure 2: *Material budget of ATLAS ID. The amount of material traversed by the electrons varies with pseudorapidity* η *from about 0.5 to about 1.5 radiation lengths.*

from the interaction point in the pseudorapidity range $|\eta| < 0.8$ ("barrel region") will go through the beam pipe, 3 layers of Pixel detectors, 4 layers of Semi-Conductor Tracker detectors (SCT), and 73 layers of Transition Radiation Detector (TRT) before reaching the calorimetry. Even in the barrel region, every layer of the high precision silicon detectors (Pixel and SCT) contributes 2 to 6 percent of X_0. This results in a high probability of signifi cant bremsstrahlung radiation by electrons and positrons, influencing the quality of their track reconstruction and measurement.

2. Bremsstrahlung

The "brem-ray" image of the ATLAS Inner detector (fi g. 3), which shows $R-Z$ coordinates

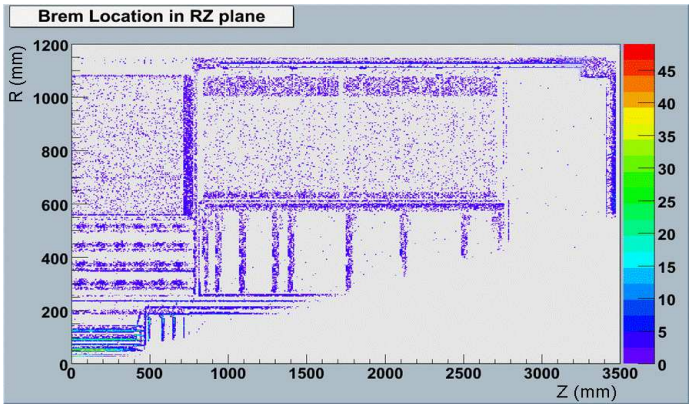

Figure 3: *The $R-Z$ coordinates of simulated bremsstrahlung points, showing that the denser parts of the inner detector account for more frequent brems, with more energy radiated.*

of simulated bremsstrahlung points, highlights the fact that denser parts of the detector account for more frequent brems, with more energy radiated. Early brems — in pixel and lower silicon layers — make electron momentum measurement ever more diffi cult.

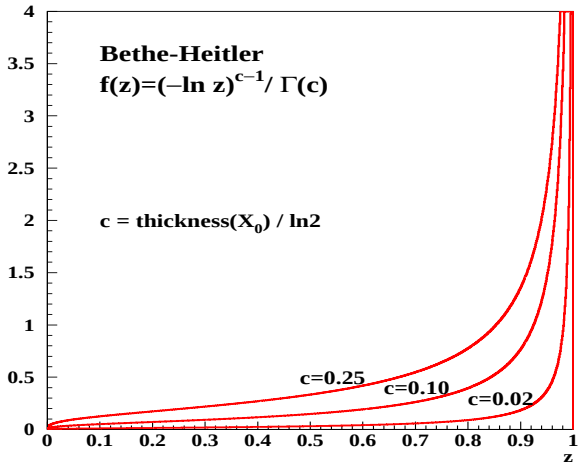

Figure 4: *Bethe-Heitler distribution of the fraction z of energy retained by the radiating electron.*

According to the description of the bremsstrahlung process [2], the electron retains its direction of propagation and a fraction z of its energy, with the probability density given by the Bethe-Heitler distribution (fig.4). This probability density $f(z)$ depends on the amount of traversed material and is highly asymmetric, with a singularity at $z \to 1$ and a long tail extending to very small z.

Fig. 5 shows a radiating track in the magnetic field. If an electron suffers an act of bremsstrahlung at point C, its track will have a smaller radius of curvature after that point, hitting layer S5 at point F instead of point G (while the photon follows the tangent C–E–H). A tracking algorithm which

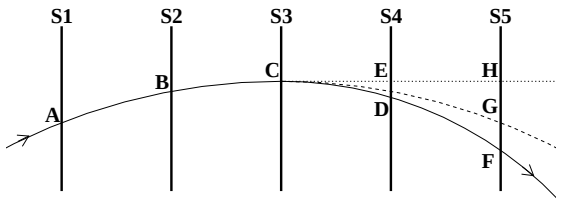

Figure 5: *A track changing its curvature at point C due to bremsstrahlung. This track has lost 35% of its momentum at that point.*

does not take the possibility of such changes into account will, in such cases, return a track with an underestimated momentum value and unacceptable fit quality.

3. Kalman Filtering

The default track reconstruction method in ATLAS [3] uses a Kalman filter (KF) [4, 5]. This is an iterative procedure used to determine the vector of track parameters, y, and its covariance matrix, C, taking into account the measurement m (and its respective covariance matrix V) at each detector layer k. In a slightly simplified notation, the procedure includes three steps:

1. Extrapolate y and C from layer $k-1$ to layer k:

$$y_{k-1} \to y_k^-, \qquad C_{k-1} + Q_{k-1} \to C_k^-$$

   Here Q_k is the covariance matrix of the system noise at layer k, which can take into account things like multiple scattering and bremsstrahlung.

2. Calculate Kalman gain K at layer k:

$$K_k = \frac{C_k^-}{C_k^- + V_k}$$

3. Do measurement update:

$$y_k = y_k^- + K_k(m_k - y_k^-), \qquad C_k = (1 - K_k)C_k^-$$

It can be shown (see e.g. [4] and references therein) that this procedure only works properly if both measurement uncertainty V and the process noise Q are well described by gaussian distributions. While this is usually the case for measurement errors and multiple scattering, it's certainly not true for bremsstrahlung, which causes problems during electron track reconstruction. As mentioned above, when applied to a radiating electron track similar to the one shown in fig. 5, the default KF fit is likely to result in a bad fit quality with an underestimated reconstructed momentum.

4. Gaussian Sum Filter

In the standard implementation, the Kalman filter can only view bremsstrahlung as another source of gaussian-distributed noise, which is clearly a very crude approximation to the Bethe-Heitler distribution (fig. 6). So, early attempts to replace the Bethe-Heitler distribution with a

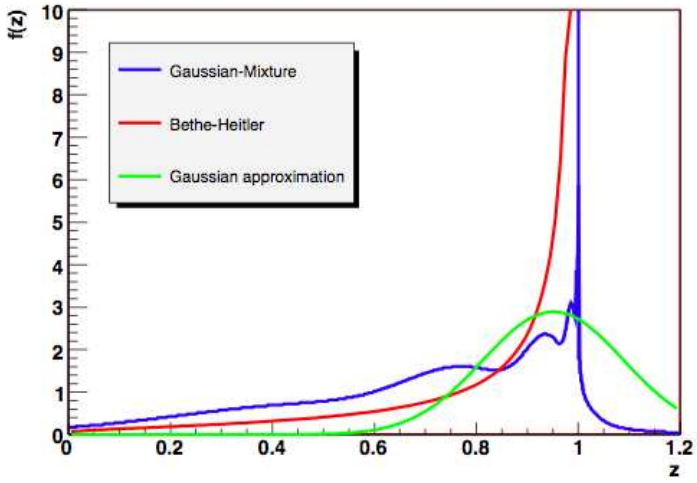

Figure 6: *Comparison between the Bethe-Heitler distribution, a single gaussian distribution of equivalent mean and r.m.s., and a sum of several gaussians used by the Gaussian Sum Filter.*

single gaussian of equivalent mean and width did not work too well.

The Gaussian Sum Filter (GSF) [4, 6] is a non-linear generalisation of the Kalman filter. GSF approximates Bethe-Heitler distribution by a mixture of several gaussians, thus allowing to take into account the asymmetry and the low-energy tail of the distribution. After that, several Kalman filters run in parallel. In order to make things manageable and avoid exponential growth of components, component reduction has to be performed at each step. Even so, GSF may take 10 or even 100 times longer than the default KF.

GSF can be quite successful in bremsstrahlung recovery — e.g., the effective track momentum resolution for 10 GeV electrons in ATLAS improves from about 10% to 8%. However, the hefty computing overhead is a major limiting factor in its use.

5. Dynamic Noise Adjustment

Another, quick and efficient method of dealing with electron tracks has been developed and

implemented in ATLAS. It is based on the Dynamic Noise Adjustment (DNA) [7] during Kalman filtering.

At each silicon layer, a simple single-parameter fit is performed to flag hits which may be associated with bremsstrahlung. This fit tries to estimate the increase in curvature due to possible bremsstrahlung at the current detector layer. If no bremsstrahlung was flagged, the track fitter reverts to the default Kalman filtering procedure. Otherwise, the result of the single parameter fit — the estimated fraction of energy retained by the electron, z — is used to calculate the additional effective "system noise" term, which is then fed to the Kalman filter.

The effective "system noise" variance calculation is illustrated by fig. 7, which shows how the Bethe-Heitler distribution is mapped onto the gaussian distribution of unit width. The deviation Δz of the estimated z from the median z_0 is mapped onto the gaussian to find the corresponding deviation Δx. The effective noise σ is then calculated as $\sigma_{\mathrm{DNA}}(z) = \Delta z/\Delta x$. This procedure is equivalent

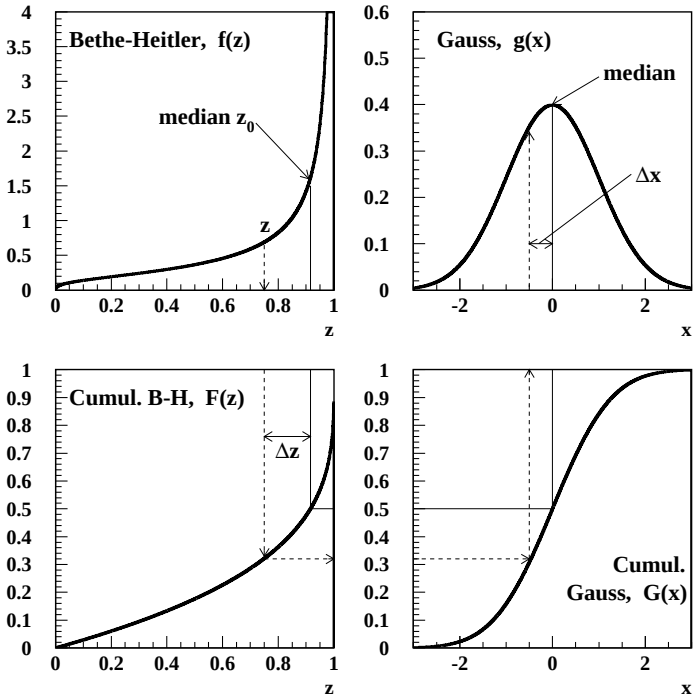

Figure 7: *Mapping of the probability distributions used to calculate the variance of the effective noise term.*

to representing the random variable z, distributed according to the Bethe-Heitler probability density, in the form

$$z = z_0 + x\,\sigma_{\mathrm{DNA}}(z)$$

where x is a random variable with gaussian probability distribution.

So, in this approach bremsstrahlung is legitimately treated as a source of *gaussian* noise, but only in those cases when bremsstrahlung-like behaviour of the track has been detected. The proper gaussian probability distribution of this "system noise" is now guaranteed by construction.

Of course, σ_{DNA} also depends on the thickness of material associated with the corresponding layer, as illustrated by Fig.8.

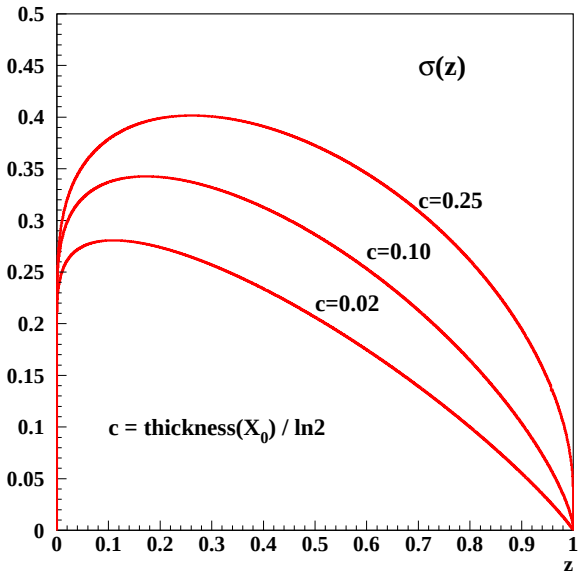

Figure 8: *Effective $\sigma_{\mathrm{DNA}}(z)$ for various values of material thickness in the detector layer.*

The variance σ^2_{DNA} is added to the appropriate term of the Kalman covariance matrix used during the fit, similarly to the treatment of any other source of system noise. However, this particular noise term is adjusted dynamically according to the estimated z and the thickness of the layer, thus justifying the name of the method.

6. DNA fit in action

The comparison between the results of the default Kalman Fit (labelled "DEFAULT", top row) and KF with DNA (labelled "DNA fit", bottom row), for a simulated sample of 20 GeV single electrons in the barrel region $|\eta| < 0.8$, is shown in Fig. 9. The left column shows the ratio of measured to generated momentum, where one can see a marked reduction of the low momentum tail and a significant improvement in the average momentum measurement. The distribution of estimated errors on measered momentum, returned by the fit (middle column), shows an increase of the errors in cases where radiation has been flagged, which is quite natural and significantly increases the percentage of reliably measured electron tracks. This is illustrated by the improvement in the pull distribution (right column) with the gaussian core now showing a mean of -0.1 and a width of 0.98 (as opposed to -0.6 and 1.09, respectively, for the default fit).

When applied to heavier particles, the DNA fit did result in some deterioration of the fit quality, and introduced some small biases, which we hope to reduce in the future. Investigation of the differences in the behaviour of the fitted momentum for electron and pion/muon tracks, with and without the DNA corrections, shows some interesting patterns, which open the possibility of separating “false positives” from true radiating electrons and may result in a useful tool for early identification of electrons.

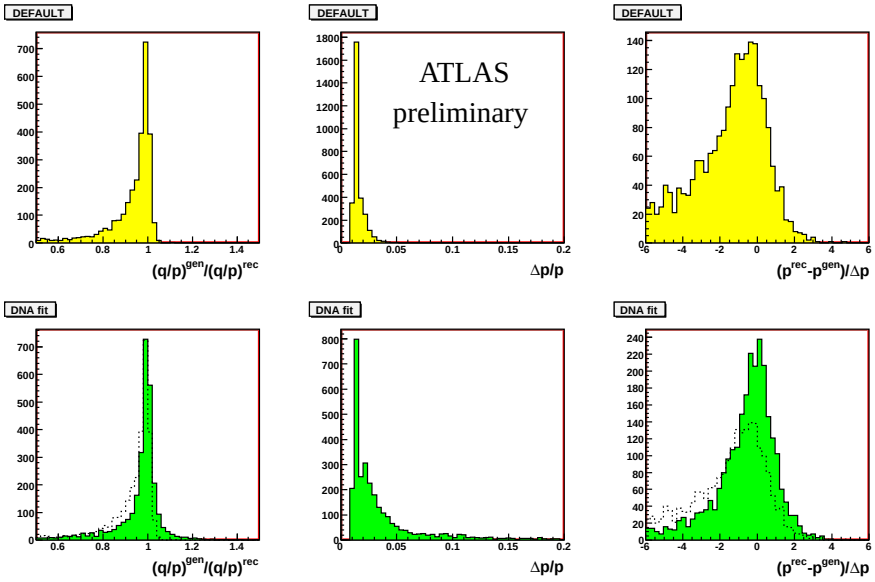

Figure 9: *Comparison of measured momentum, estimated error and pull distributions with default fit (top row) and DNA fit (bottom row) for single electron simulations at 20 GeV in the barrel region.*

Table 1 shows the comparison of the numbers of simulated electron tracks in various selections, for the default and DNA fits. Note that improved track measurement in the precision silicon layers results in better matching between the silicon and TRT track segments. This, in turn, reduces the fraction of electron tracks without TRT extensions from 20% to 8 %. This also means better extrapolation to the electromagnetic calorimeter (ECAL) and hence improved track-to-ECAL matching.

Table 1: *Fractions of electron tracks falling into various selections, for the default KF and the DNA fits.*

Selection	Default KF	with DNA
Total reconstructed tracks	99.0%	99.4%
Momentum within $\pm$50% of true	93.4%	94.5%
Momentum within $\pm$20% of true	84.2%	86.4%
Within gaussian core of q/p distr.	55.6%	65.5%
Within gaussian core of pull distr.	51.3%	71.2%
Tracks with TRT extensions	80%	92%

DNA fit only works with precision hits from silicon layers, and hence cannot help in recovering electron tracks radiating in TRT. For very high energy electrons its effectiveness is also reduced, as the curvature radii become too large. However, the results of the DNA fit can be used as a good starting point for yet another method of bremsstrahlung recovery, being currently developed in ATLAS. The latter uses the information from the matched ECAL cluster to improve the track fit, and thus can address these problem areas.

Remarkably, the computing overhead of the DNA fit is quite small, below 10% on top of the default fit. Better segment matching means fewer iterations of the Kalman fitter, thus sometimes making the DNA fit even faster than the default one. This opens the possibility of using the DNA fit during online processing in the high-level trigger, thus improving the electron trigger efficiency.

First results on full simulation and reconstruction of $J/\psi \to e^+e^-$ in B decay events (fig. 10) show a clear improvement if DNA brem recovery is performed: the 15 MeV shift of the J/ψ mass

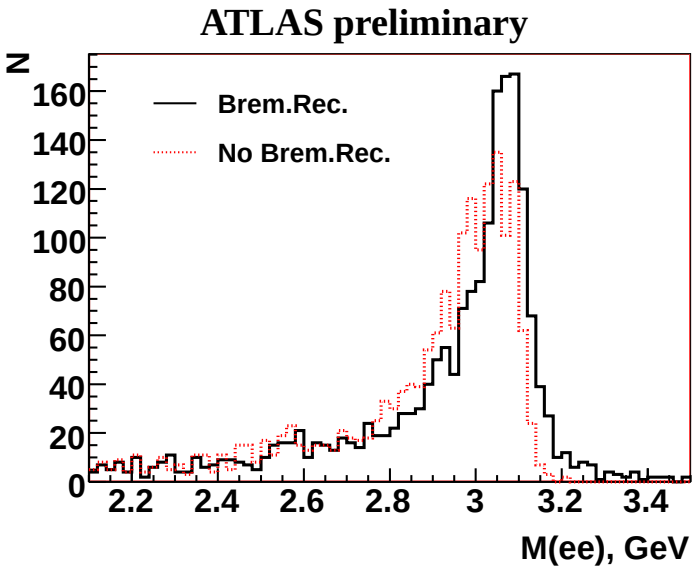

Figure 10: *Reconstructed invariant mass of e^+e^- in $B \to J/\psi(\to e^+e^-) + X$ decay events, with (solid line) and without (dashed line) bremsstrahlung recovery using the DNA fit.*

virtually disappears, invariant mass resolution is better by about 20%, and the J/ψ reconstruction efficiency is increased by 5%. It's worth noting that more reliable error estimates returned by the DNA fit play an important role in improving the fit of the secondary vertex, necessary for this analysis.

7. Conclusion

Bremsstrahlung recovery is extremely important in order to achieve the full range of physics goals in ATLAS. Higgs decays $H \to ZZ \to e^+e^-e^+e^-$ and SUSY searches in multi-leptonic final states are good examples of processes to benefit from it. Hence the number of different approaches to bremsstrahlung recovery that have been developed, tried and implemented in ATLAS.

This presentation described the track fitting procedure which uses Dynamic Noise Adjustment during the Kalman filtering process, used in ATLAS tracking. DNA fit works well: significant improvements in electron track reconstruction efficiency and quality have been achieved. Thanks to its speed, DNA fit can also be used online in high-level trigger to improve electron trigger efficiency.

DNA fit is still in development, with further tests and potential improvements in progress. For example, in some cases "early" electron identification, based on silicon hits, may become possible.

8. Acknowledgements

The author is grateful to many ATLAS colleagues who contributed to this presentation one way or another. Special thanks are due to Tom Atkinson, Anne-Catherine Le Bihan, Maria Jose Costa, Markus Elsing, Igor Gavrilenko, Jason Lee, Wolfgang Liebig, Darren Price and Andreas Salzburger.

References

[1] ATLAS Detector and Physics Performance TDR, CERN/LHCC 99-14, Geneva, May 1999.

[2] H. Bethe, W. Heitler, *Proc. Roy. Soc. Lond.* **A146** (1934) 83.

[3] ATLAS tracking event data model. F. Akesson et al., ATL-SOFT-PUB-2006-004, CERN, Geneva, July 2006.

[4] Branko Ristic, Sanjeev Arulampalam, and Neil Gordon, "Beyond the Kalman Filter: Particle Filters for Tracking Applications", Artech House, 2004.

[5] R. Frühwirth, *Nucl. Instr. Meth.* **A262** (1987) 444.

[6] R. Frühwirth, *Comp. Phys. Comm.* **100** (1997) 1.

[7] V. Kartvelishvili, "Electron bremsstrahlung recovery in ATLAS", talk given at IPRD06, 1–5 October 2006, Siena, Italy.